

# Rapid Detection of Nitrofurantoin and Its Metabolites by Using Carboxylic Multi-walled Carbon Nanotubes Modified Glassy Carbon Electrode

Baoshan He\*, Ming Li

School of Food Science and Technology, Henan University of Technology, Zhengzhou 450001, People's Republic of China

\*E-mail: [hebaoshan@126.com](mailto:hebaoshan@126.com)

Received: 8 January 2018 / Accepted: 4 March 2018 / Published: 10 April 2018

---

An electrochemical method using carboxylic multi-walled carbon nanotubes (MWCNTs-COOH) modified glassy carbon electrode (GCE) was described for detecting nitrofurantoin (NF) and semicarbazide (SEM) residual. The chemical structure and morphological features of carboxylic multi-walled carbon nanotubes were determined by FTIR spectroscopy and scanning electron microscope. The electrochemical behavior of NF and SEM on MWCNTs-COOH/GCE was also investigated by cyclic voltammetry (CV). And the effect of the buffer pH and scan rate was optimized. Under the optimized experimental conditions, the linear relationship between the peak current and the concentration of NF and SEM was determined using the amperometry (AMP). The linear relationship of NF was  $I_p(\mu A) = -21.050 - 0.095c(\mu mol L^{-1})$ ,  $r = 0.999$ , with a detection limit of  $2.24 \times 10^{-7} mol L^{-1}$  (S/N=3). The linear relationship of SEM was  $I_p(\mu A) = -0.269 + 0.0599c(mol L^{-1})$ ,  $r = 0.998$ , with a detection limit of  $1.88 \times 10^{-7} mol L^{-1}$  (S/N=3). Finally, the modified electrode was successfully applied in the real sample and the average recoveries for NF and SEM were 91.1~94.0% and 92.9~98.0%, respectively.

---

**Keywords:** Carboxylic multi-walled carbon nanotubes; Nitrofurantoin; Semicarbazide; Glassy carbon electrode

## 1. INTRODUCTION

Nitrofurans (NFs), a group of synthetic broad-spectrum antibiotics, have been widely used in farming and aquaculture. Nitrofurans have obvious effects on the prevention and treatment of animal diseases, but their drug residues pose a serious threat to people's health [1, 2]. Long-term consumption of foods containing nitrofurans will cause side effects on human body. Nitrofurans are very unstable in nature and rapidly metabolize to semicarbazides (SEM), 3-amino-2-oxazolidinyl ketones (AOZ), 3-

amino-5-methylm-morpholino-2-oxazolidinone (AMOZ) and other metabolites [3-5]. And their metabolites can be combined with the protein and exist of long-term stability, causing teratogenic and mutagenic effects, which seriously endangering human health. At present, the use of NFs in food-producing animals has thus been forbidden in several countries and regions with the aim of avoiding harmful effects on human health [6-9]. However, due to their low price and significant efficacy, they have been used by lawless elements in livestock, poultry and aquaculture. NFs and their metabolites are still being detected continuously [10]. Therefore, it's an urgent task to find a fast and effective method to detect and control the NFs and their metabolites in food.

Various analytical methods such as high-performance liquid chromatography (HPLC) [11, 12], high performance liquid chromatography-mass spectrometry (LC-MS) [13, 14], high performance liquid chromatography-tandem mass spectrometry (LC-MS/MS) [15, 16], colloidal gold immunoassay [17] and enzyme-linked immunosorbent assay (ELISA) [18] have been reported for the detection of NFs and their metabolites. Although these methods can achieve satisfactory results, they usually require expensive equipments, professionals to operate and high cost [19]. It's well-known that electrochemical analysis methods are reputable with the advantages of fast, sensitive, inexpensive, easy to operate and other advantages of concern [20]. Currently, the use of electrochemical detection of NFs and its metabolites is relatively poorly reported. He [21] etc. designed a novel electrochemical sensor for the detection of NF and SEM using  $\text{Fe}_3\text{O}_4/\text{Gr}/\text{GCE}$ , with the detection limits of  $2.92 \times 10^{-6}$  mol  $\text{L}^{-1}$  for NF and  $6.17 \times 10^{-7}$  mol  $\text{L}^{-1}$  for SEM. Zhang [22] etc. studied fluorescence sensor for NF using MANPK as sensing carrier, with a detection limit of  $4.5 \times 10^{-6}$  mol  $\text{L}^{-1}$ .

Since carbon nanotubes (CNTs) were discovered in 1991, they have attracted much attention due to its excellent electrical conductivity and other properties [23, 24]. Multi-walled carbon nanotubes (MWCNTs) were of interest because of their properties such as high conductivity, large surface area, fast electron transfer and biocompatibility [25, 26]. Non-carboxylated MWCNTs exist a large number of electrostatic interactions, resulting in a decrease in stability and durability of the sensor [27]. In addition, MWCNTs tend to agglomerate, affecting their dispersion in solution [28]. Compared with MWCNTs, MWCNTs-COOH have a high specific surface area, good chemical stability and compatibility [29, 30]. Thus, carboxyl functional groups (COOH) were grafted onto the surface of MWCNTs in the experiment.

In this paper, we fabricated an electrochemical sensor by using MWCNTs-COOH modified GCE. Compared with bare GCE, the MWCNTs-COOH modified electrode strongly enhanced the current of NF and SEM and thus the detection sensitivity was significantly improved. Finally, the MWCNTs-COOH/GCE was effective in the detection of NF and SEM in the real sample.

## 2. EXPERIMENTAL

### 2.1. Chemicals and reagents

Nitrofurazone (NF) was purchased from Shanghai yuanye Bio-Technology Co., Ltd. (Shanghai, China). Semicarbazide hydrochloride (SEM·HCl) was purchased from Thermo Fisher Scientific (China) Co., Ltd. (Shanghai, China). Multi-walled carbon nanotubes (MWCNTs) were supplied by Beijing Gaoke Technology Material Co., Ltd. (Beijing, China). N, N-dimethylfomamide

(DMF) were purchased from Tianjin Kernel Chemical Reagent Co., Ltd (Tianjin, China). All other chemicals are of analytical grade and double distilled water was used throughout the experiment.

## 2.2. Apparatus

All the electrochemical measurements were performed using a CHI660E electrochemical workstation (Shanghai Chen Hua Instrument Company, china) with a conventional three-electrode system comprising a working electrode (GCE), a counter electrode (Ag/AgCl) and a reference electrode (Pt wire). Fourier Transform infrared spectroscopy (FTIR) was carried out on Nicolet 6700 (Thermo Fisher Scientific, America) and scanning electron microscope (SEM) was carried out on JSM-6700F (Japan Electron Company).

## 2.3. Synthesis of MWCNTs-COOH

MWCNTs-COOH were prepared according to a mixed acid phase oxidation method [31]. Briefly, 1.0 g of MWCNTs was added to 80 mL of mixed acid ( $\text{H}_2\text{SO}_4:\text{HNO}_3=3:1$ ), and the mixture was sonicated for 12 h to oxidize until homogeneous ink was formed. Then, the solution was vacuum filtered through a 0.02  $\mu\text{m}$  polycarbonate filter and rinsed with double distilled water until the filtrate was neutral. Finally, the treated MWCNTs were dried in vacuum oven (100  $^\circ\text{C}$ , 4 h) and stored in desiccator for further use.

## 2.4. Preparation of MWCNTs-COOH modified GCE

Prior to modification, bare GCE was carefully polished with 0.3 and 0.05  $\mu\text{m}$  alumina powder to a mirror surface, sonicated in absolute ethanol and ultrapure water for 5 min to remove any adsorbed substances on the electrode surface, and then dried at room temperature. Then, 2  $\mu\text{L}$  of 0.01  $\text{g mL}^{-1}$  MWCNTs-COOH dispersed in DMF solution was dropped onto the polished GCE surface. Finally, the electrode was dried under infrared light. MWCNTs-COOH/GCE was obtained.

## 2.5. Electrochemical measurements

CV and EIS were done by using a CHI660E electrochemical workstation at room temperature. CV was performed in 1  $\text{mol L}^{-1}$  HAc-NaAc buffer. The scan rate was 0.1  $\text{V s}^{-1}$ , and the potential ranged from -1.0 to 1.0 V. EIS was carried out in a probe solution containing 0.1  $\text{mol L}^{-1}$  KCl and 10  $\text{mmol L}^{-1}$   $\text{K}_3[\text{Fe}(\text{CN})_6]/\text{K}_4[\text{Fe}(\text{CN})_6]$  redox pair with the following parameters: the frequency range 0.1~100000 Hz; alternating current amplitude 5 mV. AMP was tested in the following parameters: initial potential: -0.36 V, sampling interval: 0.01, experiment time: 600 s, sensitivity:  $1.e^{-004}$ .

### 3. RESULTS AND DISCUSSION

#### 3.1. Characterization of MWCNTs-COOH using FTIR and SEM

The FTIR spectra of MWCNTs and MWCNTs-COOH were illustrated in Fig.1. The characteristic absorption band corresponded to OH at  $3400\text{ cm}^{-1}$ . After treating the MWCNTs, there was no change among the OH. However, changes occurred at  $1574.12\text{ cm}^{-1}$  and  $1712.40\text{ cm}^{-1}$ , corresponding to C-O and C=O, which was consistent with the result of carboxylic reported in reference [28, 32]. It showed that carboxyl groups were successfully introduced to the surface of MWCNTs after mixed acid treatment.

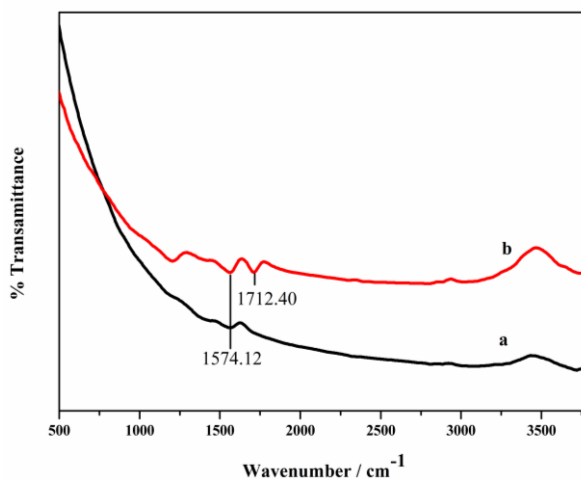


**Figure 1.** FTIR spectra of MWCNTs (a) and MWCNTs-COOH (b)

SEM image of MWCNTs and MWCNTs-COOH was shown in Fig.2. Compared with MWCNTs (Fig.2.A), the structure of MWCNTs-COOH (Fig.2.B) has changed to some extent. For example, the diameter of the MWCNTs-COOH was significantly reduced and the length was shorter. MWCNTs-COOH had larger specific surface area and higher electrocatalytic activity which were conducive to the detection of analytes. These results were similar to those of the past literatures [33-35].

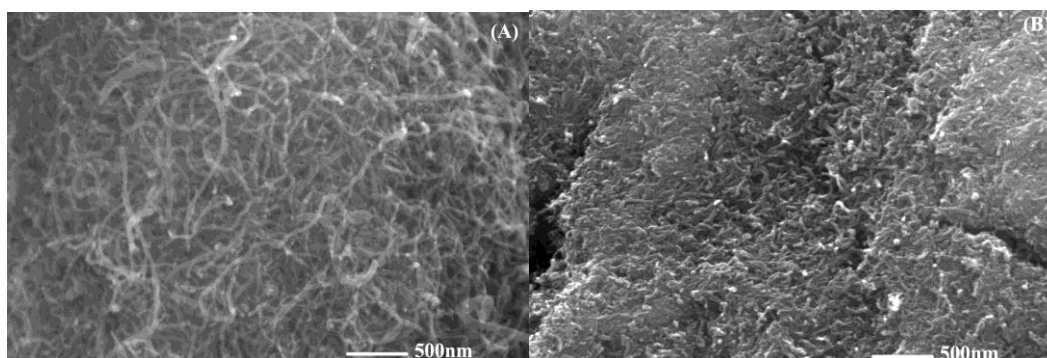


**Figure 2.** SEM image of MWCNTs (A) and MWCNTs-COOH (B)

### 3.2. Electrochemical impedance spectroscopy (EIS) behavior of GCE

To understand the characterisation of the modified electrode, the electrochemical behaviors of different modified GCE were studied by EIS. In Fig.3, arcs appearing in the high frequency region had a circular diameter corresponding to the electrode's electron transfer resistance ( $R_{et}$ ). The bare GCE exhibited a pronounced circle domain ( $R_{et} \approx 200 \Omega$ ). Curve b was the EIS graph of MWCNTs/GCE. After MWCNTs modified on GCE, the resistance of GCE was significantly reduced ( $R_{et} \approx 100 \Omega$ ), indicating MWCNTs could improve its conductivity on the surface of GCE by promoting the electron transfer rate. The semicircular diameter of MWCNTs-COOH/GCE was very small compared to MWCNTs/GCE (curve c) ( $R_{et} \approx 50 \Omega$ ). These results were consistent with these references [25, 36, 37].

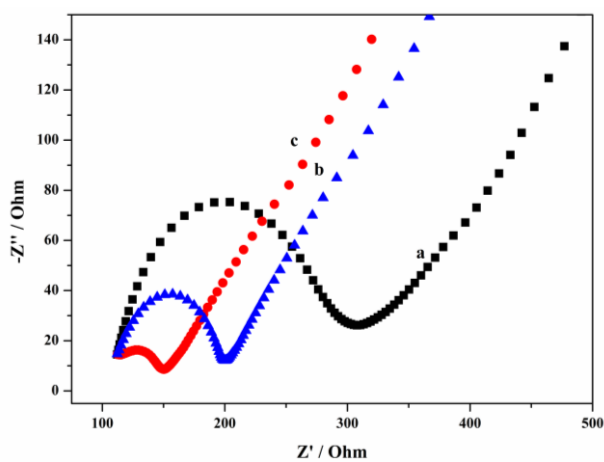


**Figure 3.** EIS of different electrodes in  $10 \text{ mmol L}^{-1} [\text{Fe}(\text{CN})_6]^{3-/4-}$  containing  $0.1 \text{ mol L}^{-1} \text{ KCl}$  (a. bare GCE; b. MWCNTs/GCE; c. MWCNTs-COOH/GCE. Frequency range:  $0.1 \sim 100000 \text{ Hz}$ . Amplitude:  $5 \text{ mV}$ .)

### 3.3. Electrochemical response of NF and SEM

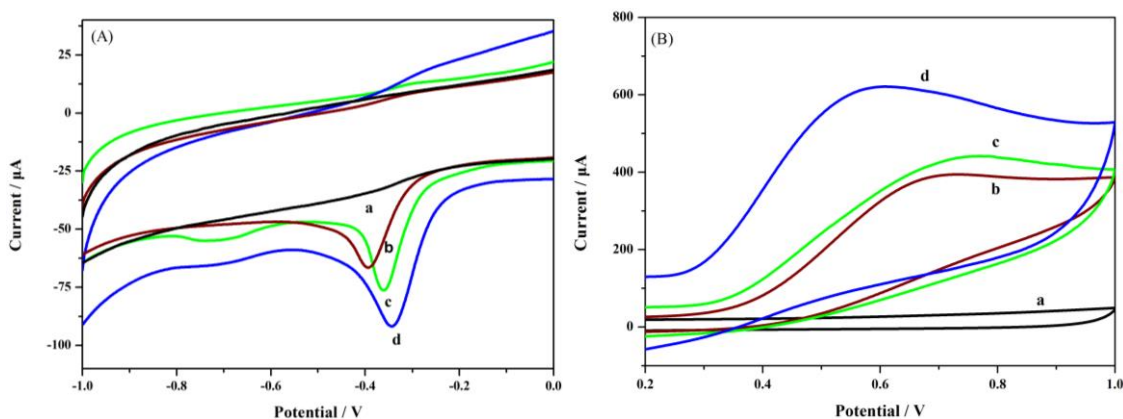


**Figure 4.** A: CV of (a) bare GCE in the absence of NF, (b) bare GCE, (c) MWCNTs/GCE, (d) MWCNTs-COOH/GCE in the presence of  $2 \times 10^{-4} \text{ mol L}^{-1} \text{ NF}$  in  $1 \text{ mol L}^{-1} \text{ HAc-NaAc}$  buffering solution ( $\text{pH} 6.0$ ), and B: (a) bare GCE in the absence of SEM, (b) bare GCE, (c) MWCNTs/GCE, (d) MWCNTs-COOH/GCE in the presence of  $1.0 \times 10^{-2} \text{ mol L}^{-1} \text{ SEM}$  in  $1 \text{ mol L}^{-1} \text{ HAc-NaAc}$  buffering solution ( $\text{pH} 6.0$ ).

CV of bare GCE, MWCNTs/GCE and MWCNTs-COOH/GCE were scanned in a  $2.0 \times 10^{-4}$  mol  $L^{-1}$  NF solution. As shown in Fig.4 (A), the reduction peak didn't appear when NF was not present in the solution (curve a). When the concentration of NF was  $2.0 \times 10^{-4}$  mol  $L^{-1}$ , a reduction peak appeared at  $-0.441$  V, the current value was  $-6.559 \times 10^{-5}$  A, indicating that electrochemical reaction occurred in NF solution (curve b). Curve c and curve d were the CV of MWCNTs/GCE and MWCNTs-COOH/GCE, the reduction peak potential and current values corresponding to  $-0.430$  V,  $-7.350 \times 10^{-5}$  A and  $-0.441$  V,  $-1.111 \times 10^{-4}$  A. Compared with bare GCE, the reduction peak current of modified GCE was significantly improved. The reduction peak current of MWCNTs-COOH/GCE was 69.39% higher than bare GCE, which was 51.16% higher than that of MWCNTs/GCE, indicating that the electrocatalytic activity of MWCNTs-COOH modified GCE was significantly increased. Then, similar situation can be seen from Fig.4 (B), when the concentration of SEM was  $1.0 \times 10^{-2}$  mol  $L^{-1}$ , the oxidation peak appeared at about  $0.730$  V for bare GCE with the current value of  $3.942 \times 10^{-4}$  A (curve b), indicating that electrochemical reaction of SEM occurred. Curve c and curve d were the CV for MWCNTs/GCE and MWCNTs-COOH/GCE of  $1.0 \times 10^{-2}$  mol  $L^{-1}$  SEM solution. It was also higher than bare GCE, when modifying MWCNTs-COOH on GCE. As a result, compared with MWCNT, the electrocatalytic efficiency of MWCNTs-COOH modified GCE was significantly increased. Therefore, MWCNTs-COOH/GCE was identified as the best electrode and used in the subsequent experiments. It showed that the experiment results were in accordance with the results of SEM and EIS analysis and were consistent with previous references [38, 39].

### 3.4. Optimization of pH

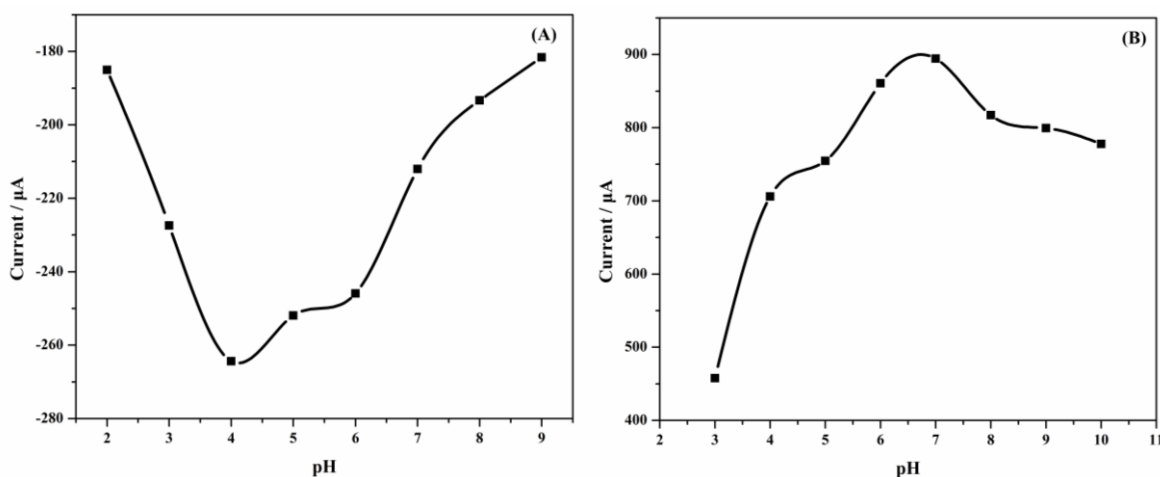


**Figure 5.** The change of peak current at different pH (A. NF; B. SEM)

In electrochemical determination, the pH of the electrolyte has a very important effect on the detection. In Fig.5, CV of MWCNTs-COOH/GCE to  $2.0 \times 10^{-4}$  mol  $L^{-1}$  NF solution and  $1.0 \times 10^{-2}$  mol  $L^{-1}$  SEM solution at different pH was shown. From Fig. 5 (A), the reduction peak current reached the maximum value at pH 4.0, indicating that the detection system was in ideal assay condition. From

Fig.5 (B), the oxidation peak current reached the highest value at pH 7.0. It could be concluded that the optimum pH for the detection of NF and SEM were pH 4.0 and pH 7.0, respectively.

### 3.5. Influence of scan rates

As shown in Fig.6 and Fig.7, CV of  $2.0 \times 10^{-4}$  mol L<sup>-1</sup> NF and  $1.0 \times 10^{-2}$  mol L<sup>-1</sup> SEM was scanned based on MWCNTs-COOH modified GCE at different scan rates. In Fig.6 (A), the scan rate ranged from 0.01 to 0.16 V s<sup>-1</sup> and the buffer pH was 4.0. Fig.6 (B) showed that the NF peak current has a linear relationship with the scan rate:  $I_p(A) = -1.31 \times 10^{-5} - 1.84 \times 10^{-4} v$  (V s<sup>-1</sup>),  $r = 0.979$ . In Fig.7 (A), the scan rate ranged from 0.01 to 0.16 V s<sup>-1</sup> and the buffer pH was 7.0.

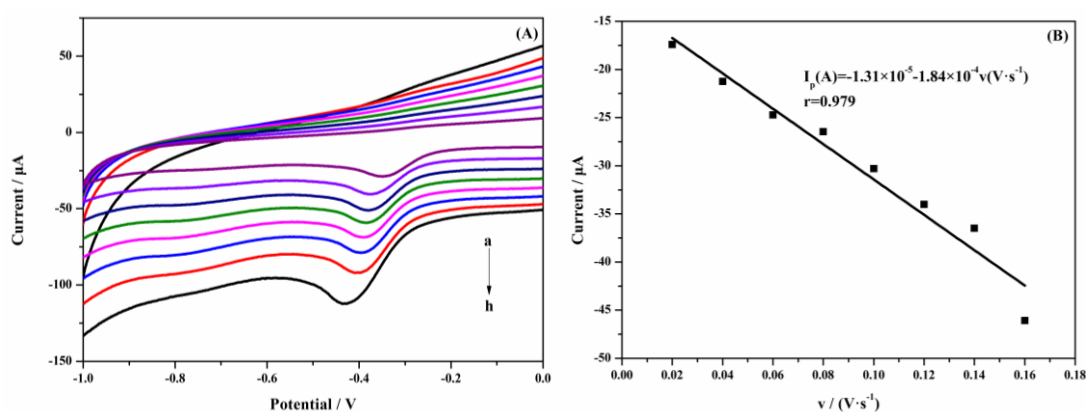


**Figure 6.** (A) CV of  $2.0 \times 10^{-4}$  mol L<sup>-1</sup> NF at different scanning rates (0.01~0.16 V/s); (B) The linear relationship between scan rates and peak current.

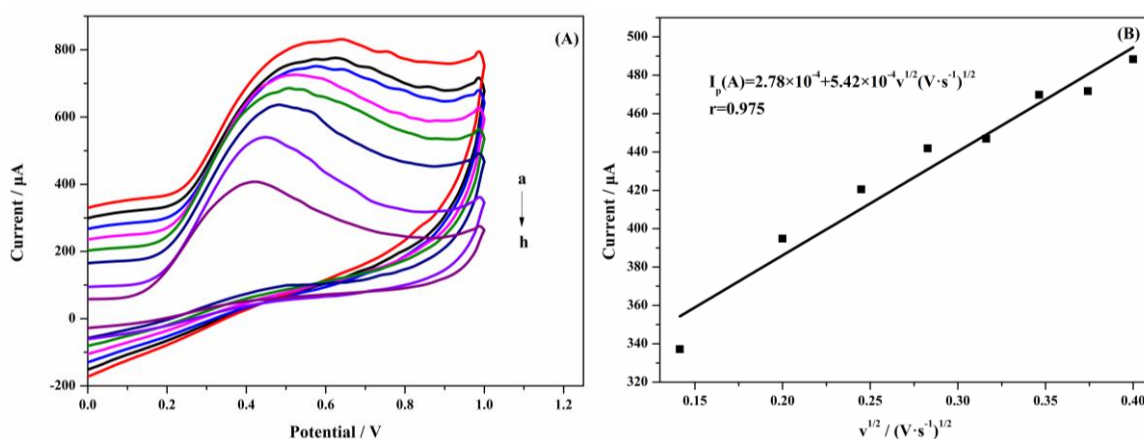


**Figure 7.** (A) CV of  $1.0 \times 10^{-2}$  mol L<sup>-1</sup> SEM at different scanning rates (0.01~0.16 V/s); (B) The linear relationship between scan rates and peak current.

This explained that the reaction of NF on the electrode was mainly affected by the diffusion control. Electroactive substances reached the electrode surface after the diffusion process, and then participated in the reaction on the electrode surface through the adsorption process. Due to the slow

electrochemical reaction and the rapid diffusion of NF, adsorption control was the control of the whole reaction. At a scan rate of  $0.1 \text{ V s}^{-1}$ , the current of NF was relatively small and had little effect on the measurement results. In addition,  $0.1 \text{ V s}^{-1}$  was chosen to measure NF as the optimal rate considering the reaction time.

From Fig.7 (B), linear relationship of the SEM oxidation peak current versus the square root of the scan rate was:  $I_p(\text{A})=2.78 \times 10^{-4}+5.42 \times 10^{-4}v^{1/2}(\text{V s}^{-1})^{1/2}$ ,  $r=0.975$ . Different from the reaction of NF on the electrode, the electrochemical reaction was relatively fast and the diffusion of SEM was relatively slow. The reaction has been completed on the surface of SEM which is involved in the electrochemical reaction. Based on factors such as reaction time and charge current, the scan rate of SEM for MWCNTs-COOH/GCE was chosen to be  $0.1 \text{ V s}^{-1}$ .

### 3.6. Electrochemical detection of NF and SEM

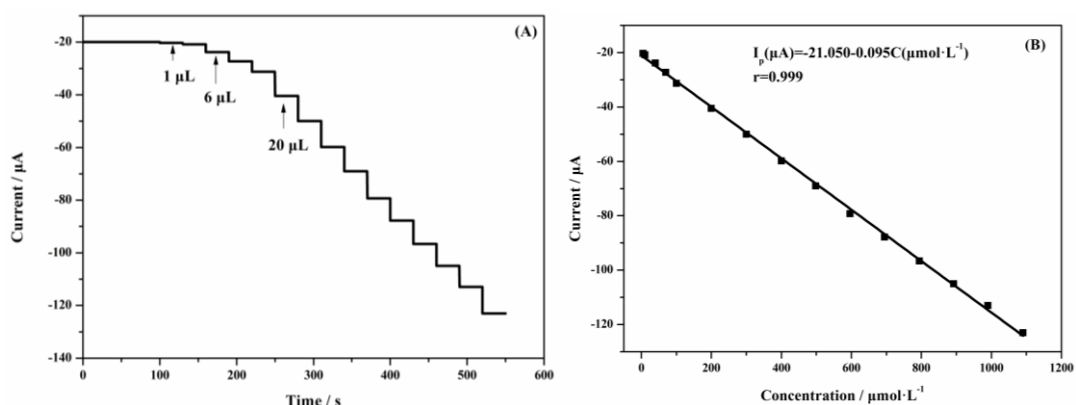


**Figure 8.** (A) Current-time plots for different concentrations of NF; (B) The corresponding calibration curve.

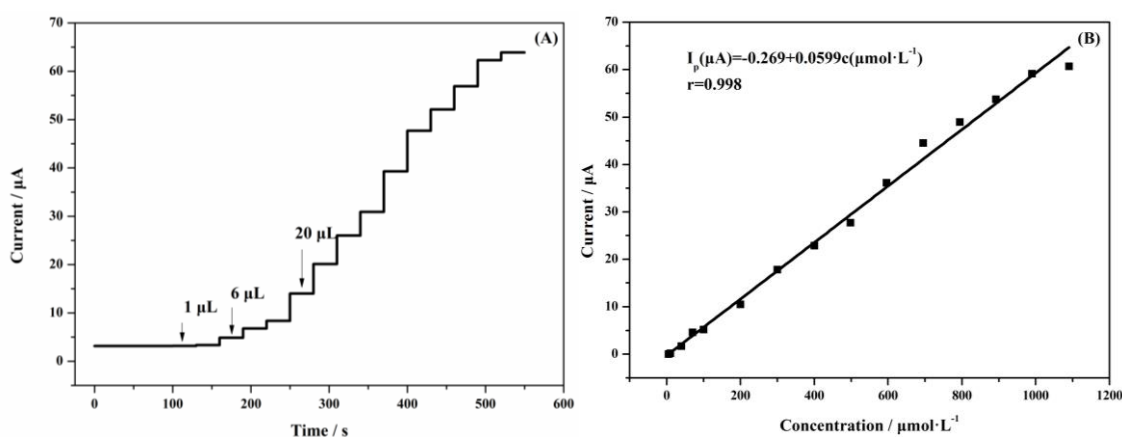


**Figure 9.** (A) Current-time plots for different concentrations of SEM; (B) The corresponding calibration curve.

The MWCNTs-COOH/GCE was used to measure NF and SEM in the range of concentration from  $5.0 \times 10^{-6} \text{ mol L}^{-1}$  to  $1.09 \times 10^{-3} \text{ mol L}^{-1}$  using amperometry (AMP). From Fig.8.(A) and Fig.9.(A), the peak current gradually increased with increasing concentration. The linear equation between NF



reduction peak current and concentration was  $I_p(\mu\text{A}) = -21.050 - 0.095c(\mu\text{mol L}^{-1})$ ,  $r=0.999$ . The detection limit of NF was  $2.24 \times 10^{-7} \text{ mol L}^{-1}$ . The linear relationship between the peak current and the concentration of SEM was:  $I_p(\text{A}) = -2.688 \times 10^{-7} + 0.0599c(\text{mol L}^{-1})$ ,  $r=0.998$ . The detection limit of SEM was  $1.88 \times 10^{-7} \text{ mol L}^{-1}$ . Compared with other methods for detecting NF and SEM, the method had a lower detection limit (Table 1) [21, 22]. The MWCNTs-COOH/GCE showed relatively high sensitivity and electrocatalytic activity.

**Table 1.** Comparison of performance of different methods for detection of SEM and NF

Modification methods	Electrochemical techniques	Target	Limit of detection ( $\mu\text{mol L}^{-1}$ )	Reference
Fe <sub>3</sub> O <sub>4</sub> /Gr/GCE	Amperometric i-t curve	NF SEM	2.920 0.617	21
MANPK (fluorescent carrier)	Fluorescence	NF	4.500	22
MWCNTs-COOH/GCE	Amperometric i-t curve	NF SEM	0.224 0.188	This work

### 3.7. Interference of coexisting substances

CV was used to determine  $0.01 \text{ mol L}^{-1}$  NF and SEM. The effects of inorganic substances, such as glucose, sucrose and organic matter, which were added 100 times, and 150 times of MgSO<sub>4</sub>, KCl, NH<sub>4</sub>Cl, CaCl<sub>2</sub> and NaCl on the current response were investigated. The results showed that RSD of the peak current before and after addition was less than 5%. It showed that the common coexists had little effect on the detection of NF and SEM by MWCNTs-COOH/GCE and could be applied to the actual detection of nitrofurantoin drugs.

### 3.8. Analysis of NF and SEM samples

**Table 2.** Detection results of of NF spiked in real pig liver samples by MWCNTs-COOH/GCE (n = 3)

Sample (NF)	Added ( $\mu\text{mol L}^{-1}$ )	Founded ( $\mu\text{mol L}^{-1}$ )	Recovery (%)	RSD (% , n = 3)
1	20.0	18.5	92.5	2.28
2	40.0	37.6	94.0	1.62
3	60.0	54.7	91.1	4.32

Based on the three-electrode working system, the actual samples of pig liver were spiked with MWCNTs-COOH/GCE. As shown in Table 1 and Table 2, NF and SEM were not detected in the

actual samples. The recoveries of three levels of NF and SEM were 91.1~94.0%, 92.9~98.0%, respectively. Therefore, the strategy can be used to detect actual sample.

**Table 3.** Detection results of SEM spiked in real pig liver samples by MWCNTs-COOH/GCE (n = 3)

Sample (SEM)	Added ( $\mu\text{mol L}^{-1}$ )	Founded ( $\mu\text{mol L}^{-1}$ )	Recovery (%)	RSD (% , n = 3)
1	20.0	19.3	96.5	3.80
2	40.0	37.1	92.9	0.97
3	60.0	58.8	98.0	2.90

#### 4. CONCLUSIONS

To summarize, a simple and sensitive electrochemical analytical method for detection of NF and SEM has been established successfully. With the assistance of MWCNTs-COOH, the electrochemical measurement signal could be enhanced sharply. MWCNTs-COOH/GCE exhibits superior performance such as low detection limit, higher sensitivity. The proposed method is expected to the application in the detection of real sample.

#### ACKNOWLEDGEMENTS

This work was supported by National Natural Science Foundation of China (Grant No. 61301037), Foundation of Henan Educational Committee (Grant No. 13A550194), Cultivation Plan for Young Core Teachers in Universities of Henan Province (No. 2017GGJS072), Key Project of Zhengzhou (Grant No. 20120663), Plan for Scientific Innovation Talent of Henan University of Technology (Grant No. 2012CXRC02), Fundamental Research Funds for the Henan Provincial Colleges and Universities (Grant No. 2014YWQQ05), Youth Backbone Teacher Training Program of Henan University of Technology.

#### References

1. A. Kaufmann, P. Butcher, K. Maden, *Analytica Chimica Acta*, 862 (2015) 41-52.
2. Y. Zhang, H. Qiao, C. Chen, Z. Wang, X. Xia, *Food Chemistry*, 192 (2016) 612-7.
3. R. Fernando, D. M. S. Munasinghe, A. R. C. Gunasena, P. Abeynayake, *Food Control*, 72 (2017) 300-305.
4. C. A. L. D. L. Torre, J. E. Blanco, J. T. Silva, *Arquivos Do Instituto Biológico*, 82 (2015) 1.
5. J. L. Meng, X. Zhou, B. Q. Zheng, J. M. Zhang, *Food Industry*, (2016).
6. S. P. Mi, K.T. Kim, J. S. Kang, *Journal of Chromatography B Analytical Technologies in the Biomedical & Life Sciences*, 1046 (2017) 172.
7. D. Wilasinee, P. Sutthivaiyakit, S. Sutthivaiyakit, *Analytical Letters*, 48 (2015) 1979-1987.
8. Y. B. Zhang, T. L. Yue, H. O. Qiao, *Journal of Northwest A & F University*, (2015).
9. A. Guzmán, L. Agüí, M. Pedrero, P. Yáñez-Sedeño, J. Pingarrón, *Electroanalysis*, 16 (2010) 1763-1770.

10. M. M. Wang, X. U. Na, Y. Tang, Z. J. Liu, *China Animal Husbandry & Veterinary Medicine*, (2016).
11. X. Y. Huang, D. M. Huang, Y. F. Shi, *Advanced Materials Research*, 554-556 (2012) 1013-1016.
12. X. Y. Huang, L. I. Bing, Y. Q. Cai, *Chinese Journal of Analysis Laboratory*, 32 (2013) 44-49.
13. L. Lin, H. Lin, X. Liu, *Chinese Journal of Analytical Chemistry*, 33 (2005) 707-710.
14. A. C. Valsecchi, L. Molognoni, N. C. D. Souza, *Journal of Chromatography B Analytical Technologies in the Biomedical & Life Sciences*, 1053 (2017) 48.
15. X. Xia, X. Li, S. Zhang, *Journal of Chromatography A*, 1208 (2008) 101-108.
16. M. Cronly, P. Behan, B. Foley, E. Malone, L. Regan, *Journal of Chromatography A*, 1216 (2009) 8101-8109.
17. X. H. Pan, Y. F. Deng, J. T. Li, *Chinese Journal of Health Laboratory Technology*, (2011).
18. T. Chungwei, H. Chihsin, W. H. Wang, *Journal of the Chinese Chemical Society*, 56 (2013) 581-588.
19. J. Borowiec, L. Wei, L. Zhu, *Analytical Methods*, 4 (2012) 444-448.
20. X. Zhang, X. Gu, K. Qu, C. Zhao, *Journal of the Chinese Chemical Society*, 61 (2014) 687-694.
21. B. He, *International Journal of Electrochemical Science*, 11 (2016) 8546-8560.
22. F. Zhang, H. Yao, T. Chu, *Chemistry*, 23 (2017) 10293-10300.
23. S. Iijima, *Nature*, 354 (1991) 56-58.
24. J. E. Park, Y. S. Jang, I. S. Park, *Advanced Composite Materials*, (2017):1-13.
25. Y. Umasankar, B. Unnikrishnan, S. M. Chen, T. W. Ting, *International Journal of Electrochemical Science*, 7 (2012) 484-498.
26. M. M. Aghayizadeh, N. Nasirizadeh, S. M. Bidoki, *International Journal of Electrochemical Science*, 8 (2013) 8848-8862.
27. C. Singh, S. Srivastava, M. A. Ali, *Sensors & Actuators B Chemical*, 185 (2013) 258-264.
28. T. Li, *New Chemical Materials*, (2013).
29. B. Deiminiat, G. H. Rounaghi, M. H. Arbab-Zavar, *Sensors & Actuators B Chemical*, 242 (2017) 158-166.
30. B. He, W. Chen, *International Journal of Electrochemical Science*, 10 (2014) 4335-4345.
31. H. X. Luo, Z. J. Shi, N. Q. Li, Z. N. Gu, Q. K. Zhuang, *Analytical Chemistry*, 73 (2001) 915-920.
32. S. A. Ntim, O. Sae-Khow, *Journal of Colloid & Interface Science*, 355 (2011) 383-388.
33. C. Zhou, S. Wang, Q. Zhuang, Z. Han, *Carbon*, 46(2008) 1232-1240.
34. G. W. Lee, J. Kim, J. Yoon, J. S. Bae, B. C. Shin, *Thin Solid Films*, 516 (2008) 5781-5784.
35. A. Varzi, C. Täubert, M. Wohlfahrt, *Electrochimica Acta*, 78 (2012) 17-26.
36. S. Tursynbolat, Y. Bakytkarim, J. Huang, L. Wang, *Journal of Pharmaceutical Analysis*, (2017).
37. H. W. Qin, X. M. Song, *Applied Chemical Industry*, 46 (2017), 2048-2052.
38. I. G. Casella, M. Contursi, *Sensor & Actuator B Chemical*, 208 (2015), 25-31.
39. C. S. Reddy, S. J. Reddy, *Electroanalysis*, 4 (2010), 595-599.